Highly scalable and flexible RNA diagnostics with One-Seq

Mingjie Dai[1,2,*], Wenzhe Ma[1], Hong Kang[1], Matthew Sonnett[1], George M. Church[2,3,*], Marc W. Kirschner[1,*]

[1] Department of Systems Biology, Harvard Medical School, Boston, MA, 02115, USA
[2] Wyss Institute for Biologically Inspired Engineering, Harvard University, Boston, MA, 02115, USA
[3] Department of Genetics, Harvard Medical School, Boston, MA, 02115, USA
*Email: mingjie_dai@hms.harvard.edu, gchurch@genetics.med.harvard.edu, marc@hms.harvard.edu

Abstract

Highly scalable molecular diagnostics is essential for effective pandemic control and prevention. Next-generation sequencing (NGS) promises highly multiplexed testing as well as viral sequencing, however current methods require complex pre-processing steps (e.g. RNA extraction and individual RT-PCR reactions). Here we report a new method, One-Seq, that allows immediate sample pooling after collection, thus enabling highly scalable testing. Specifically, we introduced a one-step reaction system to eliminate RNA extraction without compromising sensitivity, and a molecular protector strategy to eliminate individual RT-PCR reactions but still allow accurate readout, despite a large dynamic range in the sample pool. In COVID clinical specimens, our method demonstrated multiplexed testing with quantitative readout and a wide dynamic range (6 logs), sensitive detection of positive samples (Ct<35) down to 360 gce/ml, and simultaneous reports targeted viral sequences for variant identification. Our method is highly sensitive (LoD = 5 gce), highly scalable (estimated 200,000-350,000 tests per day on a high-throughput sequencer), affordable (<$1 amortized cost) and fast (8-15 hr turn-around time). We envision that our method can be ultimately implemented for whole-population, multi-virus surveillance, allowing for effective pandemic control, as well as early warning of emerging infectious viruses, preventing the next global outbreak.

Introduction

Compared to RT-qPCR based molecular tests, next-generation sequencing (NGS) promises not only highly scalable and affordable viral diagnostics, but also viral sequencing capability, both of which are critical for an effective pandemic response[1-4] as well as vaccine development[5]. The capacity for population-wide, multi-virus and variance surveillance further promises a future of "bio-weather map", where emergent infectious agents could be quickly identified and hence extinguished at the source, preventing global spread. Current high-sensitivity NGS tests[6-11] (e.g. Swab-seq, COVID-seq, LamPORE) require complex pre-processing steps before samples can be pooled, which bottlenecks the testing throughput. Specifically, two pre-processing steps are typically required for any high-sensitivity test: an RT-PCR step that performs patient barcoding as well as viral signal amplification, and an RNA extraction step that improves detection sensitivity by 20~50-fold[6,13,14]. Both steps need to be performed individually (i.e. in separate tubes), which requires complex sample and reagent handling, and practically limits the testing throughput.

To overcome this limitation and allow full scalability of NGS platforms, we developed a new, streamlined test workflow that eliminates all individual processing steps and allows immediate sample pooling after collection (Fig. 1a-b, S1a-b). To achieve this, we made two innovations. First, we developed a new sample processing protocol in which viral reverse transcription (RT) and PCR amplification steps are separated. Taking advantage of the more robust reverse transcriptase enzymes, we introduced a "one-step" composite reaction, that performs three tasks in a single tube: viral lysis, RNA preservation, and reverse transcription with patient-specific barcode. Notably, this "one-step" reaction can perform viral reverse transcription with close-to-maximum sensitivity in clinical specimens, without requiring an RNA extraction step. Second, we developed a molecular "protector" strategy that effectively suppresses barcode crosstalk during pooled PCR amplification and preserves a high dynamic range in the pooled patient samples. This method thus allows the pooling of a large number of samples before amplification, without generating false positive results. Further to enable this approach, we developed a custom sequencing construct and library preparation method, and demonstrated an effective end-to-end protocol from clinical specimen to diagnostic result. We termed this new method and detailed protocol: "One-step scalable RNA sequencing", or One-Seq for short.

We tested the performance of One-Seq in contrived and clinical SARS-CoV-2 samples. In contrived samples with pooled negative specimen background, One-Seq demonstrated high detection sensitivity on par with the most sensitive RT-qPCR tests[15-18] (200-500 gce/ml), a large and linear dynamic range (6 logs), and highly-multiplexed testing (up to 960 barcodes). In remnant clinical specimens, One-Seq demonstrated consistent high sensitivity of detection (down to 360 gce/ml) and a large dynamic range. We then investigated the compatibility of One-Seq with multi-primer testing. We showed that, the use of multiple primers for diagnostic testing allowed for further increased detection sensitivity. Finally, by designing primers adjacent to mutation hotspots, we showed that One-Seq readily allows targeted viral sequencing and identification of critical variants of concern.

Results

The molecular workflow of One-Seq consists of the following steps as diagrammed in Fig. 1c (and Fig. S1c): (1) reverse transcription (RT) of viral RNA to the first cDNA strand (Fig. 1d), following viral lysis, together with patient sample barcoding (patient ID), (2) pooling of up to 1,000 barcoded cDNA samples and purification to remove enzymes, buffer and unused RT primers, (3) second strand cDNA synthesis and library amplification, using a common forward primer and a locus-specific reverse primer (Fig. 1d). At this point the amplified library is prepared for next-generation sequencing. This streamlined workflow eliminates the RNA extraction step, and moves PCR amplification to the stage after sample pooling. Thus, the only step that requires handling of a large number of samples is the sample pooling step (Fig. S1a-b). This workflow is also designed to accommodate a second level of barcoding (batch ID)inside the reverse PCR primer (Fig. 1d, S2), allowing for further scaling up (to 100,000 samples), barcode error correction, or flexibility in combining small sample batches. This workflow is further compatible with multi-primer

detection and sequencing, allowing for increased detection sensitivity, targeted viral sequencing, and multi-virus detection. For clinical testing, apart from viral targeting primers, an extra RT primer against the human RNase P gene and a synthetic RNA target will also be included as positive controls (Fig. 1e).

To implement this workflow, we faced two critical challenges: (1) an efficient one-step reaction for viral RNA transcription in the presence of patient biomatrix , and (2) a faithful library amplification method in pooled samples without introducing crosstalk.

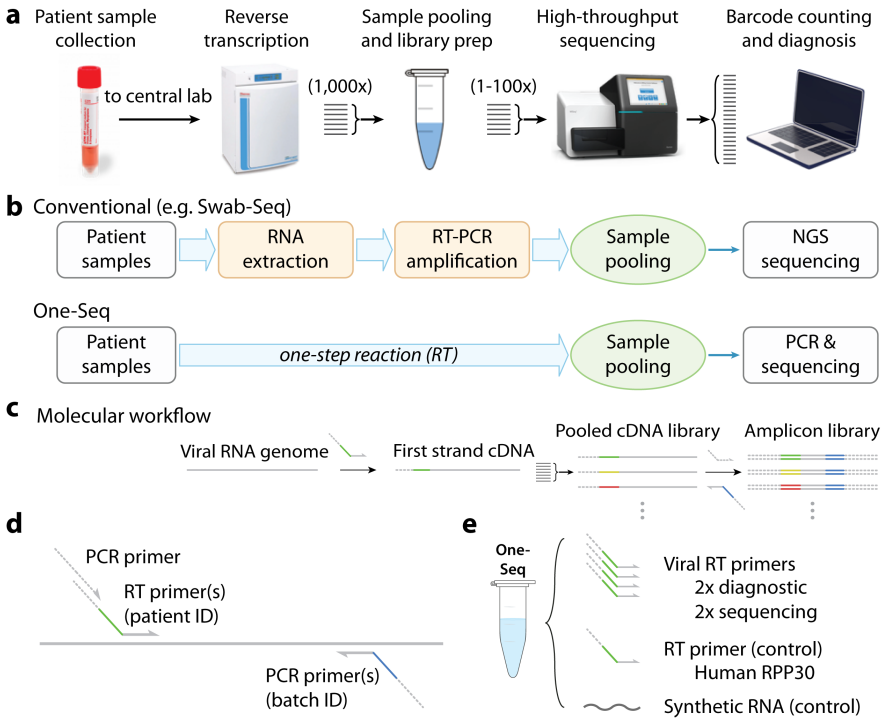


Figure 1 The principles of One-Seq for highly scalable viral testing. (**a-b**) Clinical workflow of One-Seq (a) and comparison with conventional multiplexed viral sequencing protocol (b). In (b), wide arrows indicate many individual samples; narrow arrows indicate a single, pooled sample. One-Seq eliminates all individual sample processing steps. (**c-d**) Molecular workflow (c) and primer design (d), compatible with separated RT from PCR steps. (**e**) One-Seq reaction mix for clinical testing, including multiple diagnostic and sequencing RT primers and positive controls.

One-Step reaction for efficient viral RNA transcription and sample preservation

Clinical specimens, such as nasopharyngeal (NP) swabs in viral transport medium (VTM) or saliva, are known to contain inhibitors of the RT-PCR reactions, which significantly reduce detection efficiency. To overcome this obstacle, we designed the One-Seq workflow to separate the RT and PCR steps (Fig. 1c, S1c). We reasoned that, by decoupling the two enzymatic steps, we could take advantage of the more robust reverse transcriptases as compared to polymerases, therefore have more flexibility in formulating the reaction conditions. We began our studies in contrived saliva samples, using a synthetic viral RNA spike-in (see Methods). We examined the effectiveness of different RNAse inhibitors, using an RNA degradation assay (RNaseAlert, ThermoFisher), and found that Murine (New England Biolabs) and RNAsin (Promega) provided the best and similar protection at the temperature range from 25°C to 50°C. We then compared RT efficiency of various commercial reverse transcriptase enzymes in contrived saliva samples, using qPCR readout with US CDC's RT-PCR primer and probe set[19] (see Methods), and found that SuperScript

IV reverse transcriptase outperforms the others and can detect 3 molecules of synthetic RNA in saliva background (Fig. S3a), making it a promising candidate for sensitive viral detection.

We next tested the RT efficiency and robustness of this transcriptase in contrived clinical samples, without RNA extraction (Fig. 2a, see Methods). We prepared contrived clinical samples by pooling remnant COVID-19 negative NP swab samples in VTM, and spiking in inactivated virus standard (ATCC). To assay for RT efficiency, we prepared standards in a twofold dilution series, ranging from 100 genome copy equivalent (gce) to less than 1 gce per reaction, and performed triplicate qPCR readout after incubation of the RT reaction. We found that RT products from unpurified samples indeed showed a significant inhibitory effect on PCR amplification.

We designed two new RT primers ("diagnostic primers") together with reverse PCR primers against target regions in the N gene, optimizing thermodynamic parameters and avoiding regions with significant sequence variance or homology to other related viruses (Table S1, see Methods). Following US FDA's guideline, we performed in silico primer inclusivity and specificity analysis. We found that all primers aligned to all available SARS-CoV-2 genome sequences in NCBI database (98,765 sequences, retrieved on Mar 9th 2021) with at most 1 base mismatch, with exact match to >99.4% of all sequences (Table S4). Both RT primers showed no significant (>80%) homology to genome sequences of common respiratory flora and other related viruses (Table S5). In addition, , One-Seq reads a short sequence into the viral genome, providing highly specific viral detection.

We tested the effect of detergentsin inducing viral lysis and improving RT efficiency. We found that, the addition of a mild nonionic detergent (Triton X-100) is compatible with the transcriptase, and improved the detection sensitivity by 5-fold in extraction-free samples (Fig. 2b,c, S4a). After optimization for primer concentration (Fig. S3b), we showed that both new primers allow sensitive detection of inactivated viral targets with the help of detergent (Fig. 2d, S4c), reaching a limit of detection (LoD) of 2.5 gce, close to the theoretical maximum limited by Poisson distribution. We verified our detection sensitivity with a different viral standard (SeraCare), and obtained similar results (Fig. 2d, S4c).

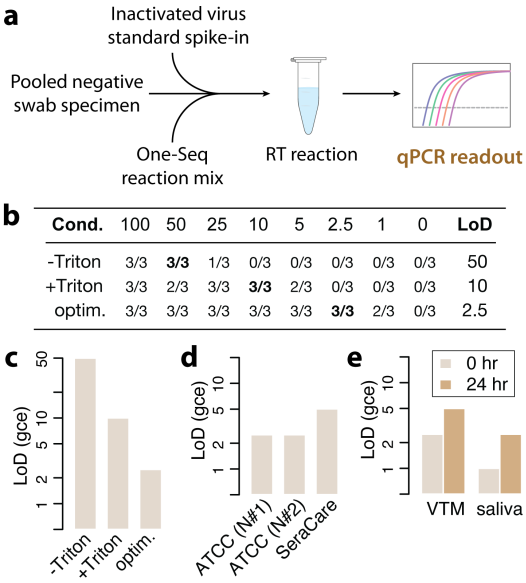


Figure 2 One-step reaction for efficient viral transcription and sample preservation. (**a**) Schematic of RT efficiency assay in contrived clinical samples. (**b-c**) Example of RT sensitivity assay using triplicate qPCR, under different conditions. LoD, limit of detection; optim., optimized condition. (**d**) RT sensitivity with different primers and viral standard. (**e**) Sample preservation assay after incubation at room temperature. VTM, viral transport medium; saliva, contrived saliva samples.

In realistic circumstances we anticipate a delay during transport of patient samples to the central testing lab (Fig. 1a), for up to 24 hr at room temperature. We thus wanted our one-step reaction system to also preserve the viral samples under such conditions. We first screened a list of potential chemicals and enzymatic agents for their effects in preserving RT efficiency. From the promising candidates, we grouped them into RNA-preserving (EDTA and DTT) and RT enzyme-preserving (antibiotic and antimycotic, protease inhibitor)

factors, and tested their effects in contrived clinical samples, as prepared above. After 24 hr incubation at room temperature, both groups showed improved RT efficiency (Fig. S3c); combined, they showed a 5-fold improved detection sensitivity (LoD = 5 gce), which is only slightly lower compared to 0 hr control (Fig. 2e, S4g-h). We also tested our RT and stabilization mix in contrived saliva samples with inactivated virus spike-in (Fig. 2e, S4g-h). Both samples (0 hr and 24 hr incubation) showed high detection sensitivity (LoD <= 2.5 gce), suggesting high RT efficiency and sample preservation in saliva samples as well.

Protector strategy for faithful library amplification without crosstalk

Clinical COVID positive specimens exhibit a large dynamic range[17,20] (up to 6-7 logs) of measurable viral load [21,22]. As a result, any barcode crosstalk during pooled library amplification could result in false positive diagnoses. To test the effect of crosstalk, we pooled RT reactions from 1~10 high-load contrived samples (equivalent to $2x10^9$ gce/ml in patient sample, or Ct=12), and supplemented them with ~90 off-target RT primers, before performing library amplification and next-generation sequencing (Fig. 3a, see Methods). Without special treatment, PCR amplification of pooled contrived RT samples resulted in an average of 0.1% barcode contamination, i.e. an upper limit of 3 logs of detectable dynamic range (Fig. 3b), much lower than what is required for accurate COVID-19 diagnostics. We hypothesized that a major contribution of the crosstalk comes from cross-hybridization of unused RT primers during the PCR amplification. Indeed, we observed higher level of crosstalk with an increase of supplemented RT primers. To overcome this problem, we designed a synthetic "protector" oligonucleotide, that consists of the RT primer (without barcode), an extended stable binding sequence to the downstream viral genome, and a polymerase blocker at the 3'-end to prevent transcription initiation (Fig. 3c). Following the principle of dynamic strand displacement[23], the protector strand would compete off any off-target RT primer from cross-hybridizing to the cDNA.

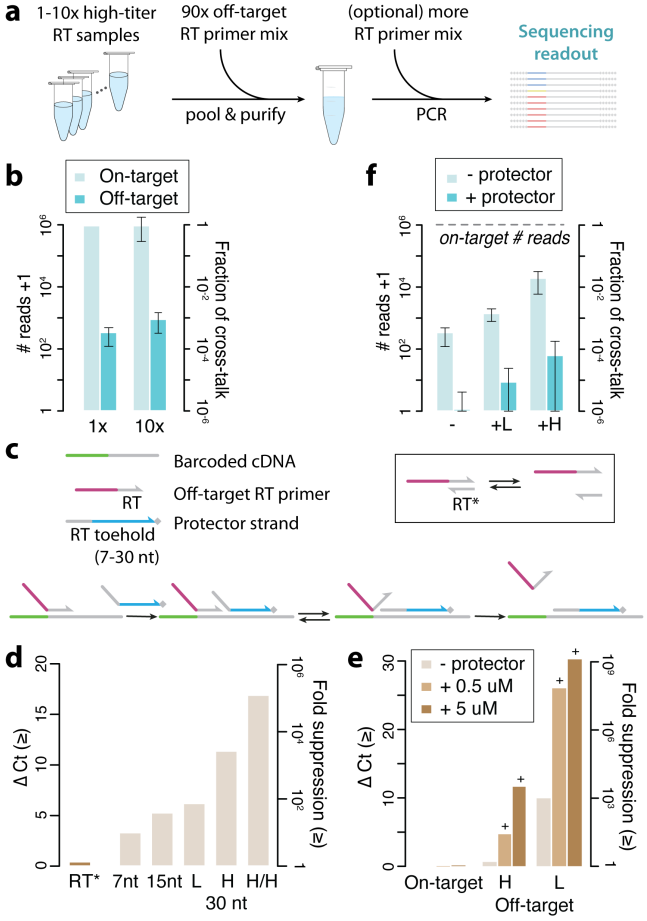


Figure 3 Protector strategy for faithful library amplification without crosstalk. (**a**) Schematic for barcode crosstalk and dynamic range test by multiplexed sequencing. (**b**) On-target and off-target sequencing reads (left axis) and fraction of crosstalk (right axis) without using protector, with 1x or 10x high-titer samples. (**c**) Protector strand design (top) and schematic for molecular mechanism of strand displacement (bottom). Insert (top-right) shows a naïve complementary strand design. RT, viral RT primer. (**d**) Suppression of qPCR amplification by different protector designs, shown as ΔCt (left axis) and fold suppression (right axis). (≥) indicates lower bounds. L, low conc.; H, high conc.; H/H, high conc. and high PCR annealing temperature. (**e**) Suppression of on-target or off-target primer amplification under different conditions. H, high conc.; L, low conc. (**f**) Suppression of off-target sequencing reads (left axis) and fraction of crosstalk (right axis) by protector strategy. -, no extra supplemented off-target primers; L, low conc. of extra primers; H, high conc.

We compared a few different protector strand designs, including a naïve approach using simply the complement of the RT primer sequence (Fig. 3c), using a single amplicon and under high RT primer concentration (see Methods). We observed that adding protector strand significantly delayed qPCR amplification, and longer toehold lengths (up to 30 nt) provided more stable binding, leading to more effective suppression (Fig. 3d, S5a). Increasing protector strand concentration and raising annealing temperature also each improved the suppression effect, as both favor the binding of the protector strand compared to that of the off-target primer. We further tested the effect of lowered RT primer concentration, as expected after cDNA purification from pooled samples (Fig. 3e). Indeed, each of these factors further reduced barcode crosstalk by 100~1,000-fold; combined, we achieved an overall 10^9-fold suppression compared to naïve PCR amplification.

We then tested our protector method with the multiplexed sequencing workflow and in contrived clinical samples, prepared as above. To further stress test our method, we also supplemented extra off-target RT primer mix directly into the PCR reaction. Our results showed that, across all conditions, addition of the protector strand significantly reduced the level of barcode crosstalk (by 100~1,000-fold, Fig. 3f). We then compared the effects of using different cDNA purification methods (Fig. S5), and found that purification using magnetic beads (e.g. Thermo MagMax kit) allowed more efficient removal of RT primers and a lower level of barcode crosstalk compared to spin columns (e.g. QIAquick PCR purification kit), potentially due to a sharper size selection cut-off. With the optimized purification and protector strategies, we significantly suppressed barcode crosstalk to a level of 0.001%. Notably, since our test was conducted under extreme conditions (1~10 sample spike-in at Ct=12), we expect a much lower level of barcode crosstalk in practical scenarios (highest viral load of Ct~15), allowing for a dynamic range of 6-7 logs, and faithful SARS-CoV-2 viral diagnosis.

Highly-multiplexed sequencing

For highly-multiplexed sequencing, we designed a custom sequencing construct that is (i) compatible with the two-stage RT-then-PCR workflow, (ii) streamlines library preparation procedure, and also (iii) minimizes sequencing runtime. To this end, we designed two custom sequencing read primers, with a short PCR adapter sequence inside the first read primer, to allow pooled amplification using a common PCR primer and be compatible with the protector strategy (Fig. S2, Table S1).

We next designed and a large set of error-tolerant samples barcodes, starting with the IDT for Illumina unique dual (UD) index sets that has the added benefit of being color balanced for Illumina sequencing platform. We expanded the set into 960 unique barcodes by concatenating both indices and inserting three short tags (Fig. 4a, Table S2). Our barcodes have a minimum pairwise Hamming distance of 12, thus are robust to a high degree of polymerase and sequencing errors (e.g. up to 6 substitutions). Without careful optimization of sequence motifs and secondary structure, our barcodes already showed highly-multiplexed (960x) detection and linear readout in contrived saliva samples (Fig. S6b). We selected a subset of barcodes that showed consistent and higher-than-average reads in two repeat experiments, and used them for subsequent tests (Fig. 4b, S6a).

To determine the multiplexed detection sensitivity of our method, we fist performed a preliminary study with a twofold dilution series, in contrived clinical samples (see Methods). In contrast to traditional RT-qPCR assays, we assigned different barcodes for different viral titer standards and replicates (e.g. three distinct barcodes per condition), and pooled all samples for library preparation and sequencing. Using the selected barcodes from above (Table S3), we measured a preliminary limit of detection (LoD) of 12 gce (Fig. S6c-d), suggesting a 2~5-fold sample loss or degradation during the cDNA purification, library amplification and sequencing steps. We then performed a confirmatory sensitivity test by repeating each condition 20 or more times and following FDA's 95% detection threshold. For both primers, our results showed an LoD = 20 gce (Fig. 4c, S7a,c), consistent with the preliminary studies.

Validation of One-Seq in clinical samples

We next validated the performance of One-seq in SARS-CoV-2 positive clinical specimens. We designed another RT primer targeting the human RNase P gene, as well as a synthetic RNA strand, both serving as positive controls for sample collection and the enzymatic reactions, respectively (Fig. 1d). To mimic the practical a scenario where clinical specimens are directly collected into One-Seq reaction tubes, we purchased remnant clinical samples (NP swab) that had not been heat-inactivated. We compared several commonly used sample media, and found that most (e.g. VTM, UTM, Multitrans) are compatible with One-Seq reaction, except Hologic Aptima, which contains lauryl sulfate and causes sample aggregation.

As a pilot test, we chose a set of representative COVID-19 positive specimens (NP swab in VTM) that spanned a wide range of Ct values (from 15 to 38), and applied the One-Seq sample workflow followed by NGS readout (Fig. 4d, see Methods). For this test, we used a mix of three distinct barcodes for each sample to maximize the detection sensitivity and robustness. Overall, One-Seq showed a linear and quantitative response against clinical viral load, and a wide dynamic range; furthermore, higher sample input allows higher detection sensitivity (Fig. 4e). One-Seq correctly detected SARS-CoV-2 RNA in all samples with a clinical Ct value of <35, demonstrating a dynamic range of 6 logs, with the lowest detected sample at Ct = 34.39 (360 gce/ml according to manufacture's specification)[24], suggesting a detection sensitivity that is close to the most sensitive RT-qPCR tests (200-500 gce/ml). The only three low-titer samples that were missed by our test all had single-positive Ct (i.e. two RT-qPCR tests gave opposite results, one positive, one negative), and with the single Ct >36 (<120 gce/ml). Notably, we used only 6 ul of specimen input, as compared to the typical 300 ul or more for an RT-qPCR test[25-27]. Further increasing specimen intake volume would further improve sensitivity. We then repeated this test with both COVID-19 positive and negative samples, using a single barcode per sample, and observed similar quantitative response with a clear separation between double-positive and negative samples (Fig. 4f).

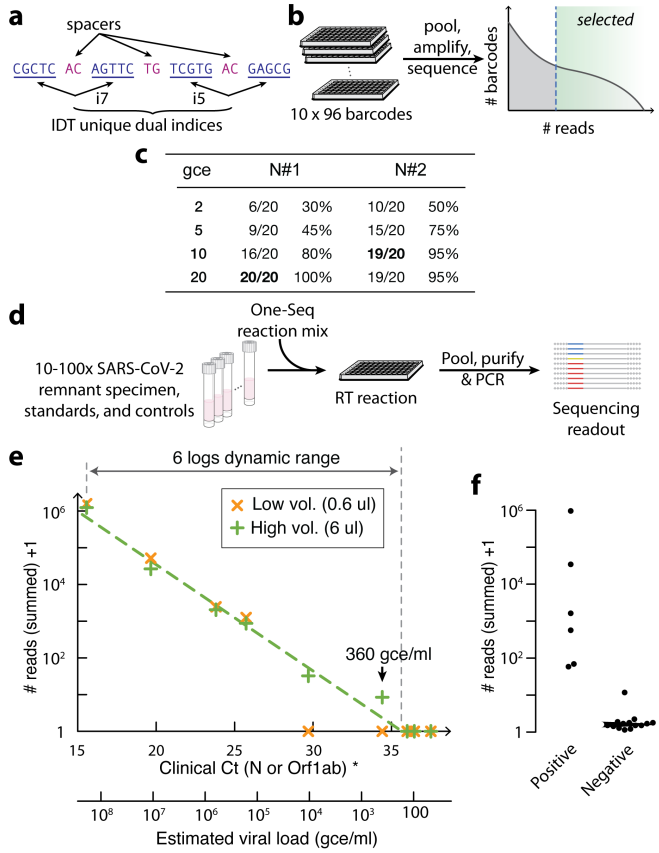


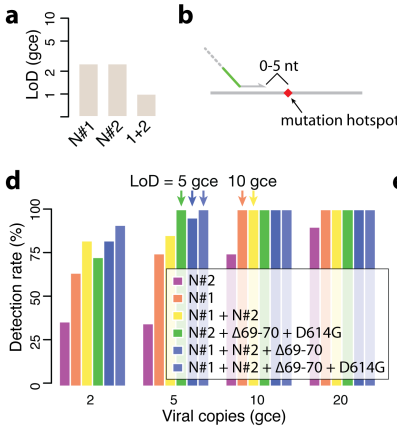
Figure 4 Multiplexed sequencing and validation in SARS-CoV-2 clinical samples. (**a-b**) Schematic of One-Seq sample barcode construction (a) and pooled selection (b). (**c**) Confirmatory sensitivity test in contrived clinical samples, using both primers. (**d**) Schematic of One-Seq validation test in remnant clinical specimens. Samples are not heat-inactivated. (**e**) One-Seq multiplexed sequencing results for SARS-CoV-2 positive clinical samples. Plot showing One-Seq reads (summed+1) against clinical Ct values (higher x axis) and estimated viral load (lower x axis, converted from Ct according to PerkinElmer IFU). (**f**) One-Seq test results for positive vs negative clinical samples.

Multi-primer detection and variant sequencing

Using multiple primer pairs simultaneously potentially gives several advantages: increased detection sensitivity, targeted viral sequencing, and multi-virus detection, all without significantly increasing cost or turn-round time. We first asked whether using two primers can significantly improve viral detection sensitivity, using a similar qPCR assay as above. Indeed, when taken together, two primers further improved RT efficiency by roughly twofold (Fig. 5a, S4d). Notably, since both primers target separate genomic loci (distance ~800 nt), the detection of both loci can be considered as independent molecular events, thus it is possible to obtain LoD values of <2 gce.

For targeted viral sequencing, we designed RT primers ("sequencing primers") in close proximity to several reported mutation hotspots in the S gene, while avoiding strong secondary structures and minimizing primer cross-interaction (Fig. 5b, S8a). After in silico analysis and a first round of qPCR test, we selected two primers against Δ69-70 and D614G mutations that showed high sequence coverage and specificity, as well as high RT sensitivity (LoD ≤5 gce) (Fig. S8b). Preliminary and confirmatory sensitivity tests in contrived clinical samples, following the same 95% detection threshold, showed similar detection sensitivity (LoD = 20 gce) as the two diagnostic primers (Fig. 5c, S7b-c). When combined, all four primers worked independently without noticeable crosstalk (Fig. S7d-e); collectively, they showed further improved detection sensitivity in multiplexed testing (LoD = 10 gce for two primers, LoD = 5 gce for three or four primers, Fig. 5d). These results suggest a clinical detection sensitivity of LoD = 250-500 gce/ml with 10-20 ul specimen intake, or down to 15 gce/ml if 300 ul specimen is used.

Finally, we asked if One-Seq with multi-primer detection can report viral mutations in clinical samples. We performed a 96x multiplexed test, consisting of 56 clinical samples (two repeats of 28 specimens), 24 contrived standards, and 16 no target controls (Fig. S9), using all four RT primers designed above (two diagnostic, two sequencing). Similar to previous test, One-Seq reported quantitative viral titer with a large dynamic range, and detected low viral titer samples (down to 360 gce/ml). Analysis of the sequenced viral genome snippets showed that D614G mutation was dominant in all positive samples tested (collected in New York, July 2020), except the inactivated virus standard (isolate USA-WA1/2020, Jan 2020), suggesting that the D614G mutation was already prevalent by July 2020 (Fig. 5e). On the other hand, we found no evidence of the del6970 mutation, consistent with the expectation that none of these samples were related to the later discovered B.1.1.7 (alpha) variant.



c

gce	Δ69-70		D614G	
2	9/20	45%	7/20	35%
5	12/20	60%	10/20	50%
10	18/20	90%	15/20	75%
20	**19/20**	95%	**19/20**	95%

e

Ct	15.6	19.6	23.8	25.7	(std)
D614G	58424	1745	162	24	9
-	36	0	1	0	129
% mut.	**99.9%**	**100%**	**99.4%**	**100%**	**6.3%**
Δ6970	2	0	0	0	0
-	17790	432	55	9	32
% mut.	**0.0%**	**0%**	**0%**	**0%**	**0%**

Figure 5 Multi-primer detection and variant sequencing. (**a**) Improvement in RT sensitivity with two primers. (**b**) Schematic for RT primer design targeting a mutation hotspot. (**c**) Confirmatory sensitivity test for two mutation-targeting primers. (**d**) Comparison of detection sensitivity with different number and combination of primers. Using three or more primers improves LoD to 5 gce. (**e**) Example of viral sequencing results for Δ69-70 and D614G primers, shown in reads (top two rows) and percentages (bottom row) harboring the specific mutation. (std), viral standard sample from ATCC/CDC.

Discussion

We report here a method for scalable viral RNA molecular diagnostics and mutation sequencing, One-Seq. By eliminating all individual sample processing steps and introducing a molecular protector strategy, One-Seq allows direct sample pooling and high dynamic range library readout, thus enabling highly scalable

multiplexed testing. Unlike recent report of multiplexed diagnostic based on isothermal amplification[28], One-Seq reports quantitative viral loads and achieves RT-qPCR-like sensitivity, on top of highly scalable testing. In COVID clinical specimens, One-Seq demonstrated multiplexed testing with a wide and linear dynamic range of 6 logs, consistently detected SARS-CoV-2 positive samples with Ct<35 and down to 360 gce/ml in viral load. One-Seq further enabled targeted sequencing at mutation hotspots, allowing for molecular diagnostics and variant identification in a single test.

One-Seq allows highly scalable testing of up to 100,000 samples per run (Table S6), while maintaining high detection sensitivity that is close to the best RT-qPCR tests. Notably, this is a scale that is comparable to the highest daily capacity from a single test center, with heavy automation and capital investment[29]. One-Seq's two-stage barcode design allows significantly reduced overhead in barcode design, manufacturing and regulatory approval, as well as flexible sample collection in smaller batches (e.g. 1,000 specimens) from local communities, organizations, or even moving vessels. One-Seq also demonstrates a higher detection sensitivity in extraction-free SARS-CoV-2 samples compared to previous reports[6,28], with a limit of detection (LoD) of 20 gce for a single primer and 5 gce when three or more primers are used. This translates to a detection sensitivity of 250-1,000 gce/ml from 5-20 ul unextracted clinical specimen, approaching the best RT-qPCR tests on the market[15,18]. Scaling up sample intake will further improve detection sensitivity, if desired. Moreover, One-Seq is affordable and has a fast turn-around time (Table S7-8). Using a high output Illumina sequencer such as the NovaSeq 6000, we estimated a sample throughput of 200,000-350,000 per day per machine, with an amortized reagent cost of <$1 and 15 hr turn-around time. Further increase in testing throughput and reduction in cost is possible with other platforms (e.g. Oxford Nanopore PromethION 48, allowing 450,000 tests per day at the same capital cost). Compared with other sequencing-based tests (Table S9), One-Seq is uniquely scalable, sensitive, and reports quantitative viral loads, thus is uniquely suited for population-wide surveillance testing.

Using multiple primers, One-Seq supports targeted viral sequencing on top of diagnostic testing, allowing variant-specific diagnosis as well as epidemiological surveillance. Compared to conventional (late pooling) methods[7,30], One-Seq's early pooling strategy together with high RT efficiency matches sequencing depth to sample abundance, thus further allowing deep sequencing and variant frequency analysis in individual samples.

In summary, we have shown that One-Seq can provide a scalable and flexible platform for viral testing (multi-virus, multi-variant), that is sensitive, affordable, and fast. One-Seq can be used for any RNA viruses, including the common cold, seasonal flu, hepatitis, dengue, Ebola, West Nile, Zika, etc. We envision that One-Seq may be ultimately implemented as a routine for whole-population, multi-virus surveillance, allowing for not only effective pandemic control, but also identification and containment of any emergent infectious agents, preventing the next global outbreak.

Methods

Clinical specimens and reference materials.

Remnant clinical nasopharyngeal (NP) swab samples (not heat-inactivated) were obtained from Boca Biolistics. Saliva samples were collected from COVID negative donors after mouth rinsing. All specimens were de-identified. The use of clinical specimen was approved by the IRB at the Harvard Faculty of Medicine. SARS-CoV-2 inactivated virus standard materials were obtained from ATCC (VR-1986HK) and SeraCare (AccuPlex 0505-0168). Viral N gene DNA template was obtained from IDT (N positive control plasmid, 10006625).

In vitro transcribed viral N gene mRNA were prepared with Invitrogen MAXIscript T7 transcription kit (ThermoFisher, AM1312), following manufacturer's protocol. The template DNA was prepared from N gene positive control plasmid (IDT) with a T7 promoter-containing primer, and purified from an agarose gel using QIAquick PCR purification kit (QIAGEN, 28104). Purified RNA product was quantified using a NanoDrop One device (Thermo).

Preparation of contrived samples.

For contrived saliva samples, saliva specimen were pooled (N=4) and spiked in with ATCC inactivated virus standard or in vitro transcribed viral mRNA, at specified concentrations. For contrived clinical samples, COVID negative remnant clinical specimens (NP swab) were pooled (N=15) and spiked in with ATCC or SeraCare inactivated virus standard, or in vitro transcribed viral mRNA, at specified concentrations. Serial dilution of virus standard was prepared with viral transport medium (VTM). VTM was prepared following CDC's protocol, with 2% FBS (heat-inactivated at 56℃ for 30 min, Gibco 26140079), 1x Antibiotic-Antimycotic (Gibco, 15240096) and 11 mg/L phenol red, in 1x Hank's balances salt solution (Gibco, 14025092).

Design of RT and PCR primers.

RT and PCR primers were designed with the following general principles: (i) optimize thermodynamic properties for specific hybridization and efficient transcription, (ii) maximize coverage for reported SARS-CoV-2 genome sequences, (iii) minimize homology and crosstalk with other related viral sequences, e.g. SARS and MERS. Specifically, RT primers were designed with T_m in the range of 54-60℃, and strong binding at the 3'-end; and PCR primers were designed with T_m in range of 60-62℃, and weak binding at the 3'-end. RT primers targeting mutation hotspots were design to be in close vicinity (within 5 nt) to the targeted loci, to minimize extra sequencing runtime. T_m values were calculated with IDT's oligo analyzer, using RNA/DNA-targeting primer settings for RT/PCR primers, respectively. A full list of RT and PCR primer sequences used in this study is included in Table S1.

Analysis of primer specificity and inclusivity.

In silico analysis for primer specificity and inclusivity was performed following FDA guideline (Molecular Diagnostic Template for Laboratories). Inclusivity analysis was performed against all available SARS-CoV-2 genome sequences downloaded from NCBI (98,765 sequences, retrieved on Mar 9th, 2021), after excluding incomplete genomes (sequences with consecutive N's and sequence fragments less than 20,000 nt in length). Specificity analysis was performed on Blastn against the recommended list of common respiratory flora and other viral pathogens (full list in Table S5), using parameters optimized for detection of short, somewhat similar sequences.

One-step reaction.

One-step sample reaction for viral lysis, RNA preservation and reverse transcription was performed with SuperScript IV reverse transcriptase (Thermo, 18090010) in manufacturer provided reaction buffer (without DTT), supplemented with 10% (v/v) murine RNAse inhibitor (New England Biolabs, M0314), 0.1% Triton X-100, 1x Antibiotic-Antimycotic (Gibco, 15240096), 0.5 mM EDTA, 5 mM DTT, cOmplete

protease inhibitor cocktail (1 tablet into 13.3 ml, Sigma, 11873580001), 0.5 uM poly-A60 DNA oligonucleotide, 15 ug/ml E. coli tRNA (Sigma, 10109541001), and further supplemented with 35-50% (v/v) equivalent of VTM or contrived clinical or saliva samples, and 125 nM of barcoded RT primer (for each primer). For RT sensitivity and sample preservation tests, different subsets of above components were added to the reaction mix. For primer concentration studies, 25-500 nM of barcoded RT primers were used instead.

One-step reactions were assembled on ice-cold blocks. Once assembled, the reaction was incubated at 50℃ for 30 min, followed by enzyme inactivation at 95℃ for 5 min. For sample preservation studies, the assembled reaction was incubated at room temperature (shielded from light) for up to 24 hr before starting the 50 ℃ incubation.

RT sensitivity test.

For RT sensitivity test with diagnostic primers (N#1 and N#2), qPCR was performed with 0.5-1.0 ul of one-step reaction product added to 40 ul Taq polymerase qPCR mix with standard buffer (New England Biolabs, M0273), 0.2 mM dNTP mix and CDC SARS-CoV-2 primer and probe set at 0.5 uM equivalent primer concentration (IDT RUO kit, 10006713). For RT sensitivity test with mutation targeting primers (Δ69-70 and D614G), qPCR was performed with dye-based readout, using Luna Universal qPCR Master mix (New England Biolabs, M3003) and 0.5 uM of both forward and reverse PCR primers.

qPCR samples were run on a Bio-Rad C1000 thermal cycler and CFX real-time PCR system for 50 cycles, and with melt curve analysis for dye-based readout. Ct values were determined by manufacturer's auto-thresholding function when possible. Samples were run in triplicates, and limit of detection (LoD) was determined to be the lowest viral titer at which all (3/3) tests yielded a valid Ct value. For dye-based qPCR, results were interpreted with melt curve analysis instead.

Protector strand design and off-target crosstalk tests.

DNA protector oligonucleotides were designed by concatenating the RT primer sequence, a stretch of 7-30 nt of downstream viral genome sequence (complement), and a 3' transcriptase blocker to prevent primer extension. A list of sequences for protector strands used in the study is included in Table S1. All protector strands were purchased from Integrated DNA Technologies (IDT).

For barcode crosstalk studies with multiplexed sequencing readout, one-step reaction products from 1 or 10 high-load barcoded samples were mixed and supplemented with 95 or 86 off-target RT primers (96 barcodes total), before cDNA purification, library amplification and sequencing (see below for barcode design and experimental protocols). High-load barcoded samples were prepared with in vitro transcribed viral mRNA in contrived clinical samples. After sequence analysis, on-target and off-target barcodes were counted, and off-target counts were reported after normalizing on-target count (or average on-target count) to 10^6. In Fig. 3f, extra off-target primers were supplemented at 2 nM (low conc.) or 10 nM (high conc.).

For protector strand suppression studies with qPCR readout, Luna Universal qPCR Master Mix (New England Biolabs, M3003) was mixed with a DNA template containing the RT primer sequence, an on-target or off-target RT primer, the protector strand, and a reverse PCR primer. In Fig. 3d, protector strands with different toehold length (7-30 nt) or the naïve RT primer complement was used. Protector strands were supplemented in the PCR reaction at 0.5 uM (low conc.) or 5.0 uM (high conc.), and annealing temperature was set at 50 ℃ (low), 64 ℃ (regular) or 72 ℃ (high). In Fig. 3e, on-target or control primers were supplemented at 250 nM, off-target primers were supplemented at 250 nM (high conc.) or 2.5 nM (low conc.).

Sample barcode and sequencing primer designs.

Patient sample barcodes (patient ID) were designed based on the IDT for Illumina Unique Dual Index set (Illumina), containing 4 plates of 4x96=384 sequence pairs in total. Each pair of i7 and i5 indices were concatenated and expanded by inserting of the following sequences in between blocks (Fig.

4a): …AC…TG…AC… (4x96), …CA…CT…GA (4x96), …AC…AC…TG… (2x96). Such a design ensures a minimum Hamming distance of 12 between any two barcodes and avoids any homopolymer repeats longer than 3 nucleotides. 960 unique barcodes were designed and tested in this work by taking the first 10 plates from this design. Batch sample barcodes (batch ID) were selected from the set of IDT8 NGS indices (IDT).

Custom sequencing read primers were designed to be orthogonal to Illumina P5 and P7 adapters and have T_m > 70 ℃. Additional, a short PCR adapter sequence (T_m ~ 60 ℃) was designed as a part of the read 1 primer for pooled PCR amplification.

A full list of RT and PCR primers, sequencing adapters and read primers used in this study are included in Tables S1. A list of custom unique patient barcodes are listed in Table S2, with 96 selected barcodes in Table S3. A list of selected batch barcodes are listed in Table S4.

Multiplexed test, sample pooling and cDNA purification.

For multiplexed test in contrived samples, a master mix of above one-step reaction mix without barcoded primer and contrived clinical sample was first prepared and aliquoted into a 96-well plate, then RT primers with unique barcodes and individual samples was added to each well. All samples were prepared on ice (master mix) or ice-cold blocks (plate samples) before incubation at 50 ℃, followed by enzyme inactivation at 95 ℃ for 5 min.

One-step reaction samples (either entire reaction, or a fraction of it, 10-40 ul each) were pooled by multichannel pipettes from 96-well plate(s) to a single tube, followed by cDNA purification using MagMax viral/pathogen nucleic acid isolation kit (Thermal, A42352). We adapted the manufacturer's protocols for large sample volume and high recovery sensitivity. Specifically, we used 50 ml conical tubes and introduced an extra centrifugation step (3,000 rcf for 3 min) before magnetic attraction for fast and effective collection of the beads. To ensure maximum detection sensitivity, we used low-bind tubes and pipette tips, and supplemented carrier DNA and RNA (poly-A60 oligonucleotide and E. coli tRNA) to the purified cDNA library samples.

For purification method comparison study (Fig. S), we tested several alternative methods: QIAquick PCR purification kit (QIAGEN, 28104), QIAquick nucleotide removal kit (QIAGEN, 28304), MagMax viral/pathogen nucleic acid isolation kit (Thermal, A42352), and AmPure XP beads (Beckman Coulter, A63880), all following manufacturer's protocols.

Library preparation and sequencing.

Pooled and purified cDNA library was amplified in a dUTP-containing PCR reaction, using Luna universal qPCR master mix (New England Biolabs, M3003), supplemented with 0.125-0.5 uM of each PCR primer, 2 uM of each protector strand, and UDG enzyme at 25 units/ml (New England Biolabs, M0372). For tests with a single RT primer, 0.25 uM of both forward and reverse PCR primers were used. For tests with 4 RT primers, 0.5 uM of forward (common) and 0.125 uM of each reverse (target specific) PCR primers were used.

Library amplification were run for 40-50 cycles with a custom-optimized thermocycling program. The first two cycles use a low annealing temperature at 52-58 ℃, followed by extension at 60 ℃; the rest cycles use a high annealing temperature at 68 ℃, followed by extension at 72 ℃. All cycles were performed with 20 s annealing followed by extension for 90 s.

The amplified library samples were within 200-260 bp range. After PCR amplification, library quality was assessed on agarose gel and the desired bands (200-260 bp range) was purified using QIAqiuck PCR purification kit (QIAGEN, 28104), and then quantitated using either Qubit 2.0 (Thermo) or Agilent TapeStation.

Sample libraries were then diluted to a final loading concentration of 10-20 pM, and supplemented with 15-20% Phi-X control v3 (Illumina, FC-110-3001) for sequencing on an Illumina MiSeq. Custom read

primers (see Table S1 for sequences) were spiked in following Illumina's protocol (2 ul of 100 uM R1 custom read primer into well 12, and 2 ul of R2 primer into well 14). For V2 Micro kit (300-cycle, MS-103-1002), 10 pM loading concentration and 100+100 base read lengths were used; for V3 Regular kit (150-cycle, MS-102-3001), 20 pM loading concentration and 100+68 base read lengths were used. Note that no indexing reads were included, and read lengths can be shortened to only include barcode regions for clinical tests.

To avoid template carryover contamination between consecutive sequencing runs, we performed two template line washes (using sodium hypochlorite solution, Sigma, 239305) between each run, following Illumina's protocol.

Sequencing analysis.

Sequencing results were aligned and analyzed using a custom workflow, consisting of the following steps: FASTQ generation and adapter trimming (using FASTQ Toolkit in Illumina BaseSpace), sequence alignment (using bowtie2, optimized for short seed), demultiplexing and read counting (custom scripts in MATLAB and Excel). Sequence alignment was performed separately for forward and reverse reads against all possible barcode sequences from one or multiple RT/PCR primers, and only alignments with ≤2 edit distance were counted. For viral mutation identification, both original and mutated sequences were considered, and the best match was reported. After alignment, each read pair was identified using both barcodes. Counts were added by 1 for each plotting.

Our current analysis pipeline is not yet optimized and takes about 30 min for each sequencing run, however with further effort it can be streamlined into a faster and more user-friendly workflow.

Confirmatory clinical sensitivity test.

Confirmatory clinical sensitivity tests were performed in contrived clinical samples, as detailed above, with a twofold dilution series spike-in of inactivated virus sample (ATCC), based on results from pilot sensitivity studies. All tests were performed with multiplexed sample workflow using up to 96 selected barcodes (see Table S3 for sequences). Each test concentration (including negative control) was repeated 20-22 times using distinct barcodes (each barcode was used once). Each RT/PCR primer set was tested multiple times with different batch barcode on the reverse side.
Positive calls were made based on a read threshold value calculated from the negative control samples, using the 3-σ formula (i.e. threshold = mean + 3× stdev). Confirmatory limit of detection (LoD) was then determined for each RT/PCR primer set using the 95% cut-off (e.g. 19/20 or 21/22 detection) following FDA's guideline.

Clinical positive controls.

Synthetic positive control RNA was designed to share the same RT primer as the N#1 target, but include a 8 nt sequence distinct from the viral genome and also uses a different reverse PCR primer (see Table S1 for sequences). Synthetic RNA was purchased from IDT, and spiked into all samples at a concentration of 10^4-10^5 copies/ul to provide positive control reads. Human RPP positive control RT primer was designed following similar principle to viral RT primers, with T_m in the range of 54-60℃, and strong binding at the 3'-end, and spiked into all samples at same concentration as viral RT primers.

For experiments containing positive controls (synthetic RNA, and human RPP), library amplification was performed separately for positive controls (PC) from viral targets, followed by independent normalization, to prevent inconclusive results due to a lack of PC reads.

Multiplexed test in clinical specimens.

For multiplexed test with clinical specimens, all hot samples were prepared inside a biosafety cabinet (BSC) following BSL 2+ protocols. The master mix was prepared and aliquoted beforehand, and clinical samples were individually added to each well, on ice-cold blocks. Incubation at 50 ℃ and inactivation at 95 ℃ were

performed in a heat block inside the BSC, followed by surface decontamination and another incubation at 95 ℃ for 5 min in a thermocycler once moved out of the BSC.

Multiplexed clinical specimen tests were arranged in sets of up to 96 samples each (including clinical samples, negative controls, and viral standards). Viral standard samples were included as quantitative references to compare with viral titers converted from clinical Ct values. Positive calls were made similar to in sensitivity tests, based on a read threshold value calculated from negative control samples, using the 3-σ formula (i.e. threshold = mean + 3× stdev).

References

1. Tromberg BJ, Schwetz TA, Pérez-Stable EJ, Hodes RJ, Woychik RP, Bright RA, Fleurence RL, Collins FS. Rapid Scaling Up of Covid-19 Diagnostic Testing in the United States — The NIH RADx Initiative. New England Journal of Medicine 2020;383(11):1071-1077.
2. Manabe YC, Sharfstein JS, Armstrong K. The Need for More and Better Testing for COVID-19. JAMA 2020;324(21):2153-2154.
3. Gandhi M, Yokoe DS, Havlir DV. Asymptomatic Transmission, the Achilles' Heel of Current Strategies to Control Covid-19. New England Journal of Medicine 2020;382(22):2158-2160.
4. Vandenberg O, Martiny D, Rochas O, Belkum Av, Kozlakidis Z. Considerations for diagnostic COVID-19 tests. Nature Reviews Microbiology 2021;19(3):171-183.
5. Mascola JR, Graham BS, Fauci AS. SARS-CoV-2 Viral Variants-Tackling a Moving Target. JAMA 2021.
6. Bloom JS, Sathe L, Munugala C, Jones EM, Gasperini M, Lubock NB, Yarza F, Thompson EM, Kovary KM, Park J and others. Massively scaled-up testing for SARS-CoV-2 RNA via next-generation sequencing of pooled and barcoded nasal and saliva samples. Nat Biomed Eng 2021;5(7):657-665.
7. Illumina Inc. Illumina COVIDSeq Test Instructions for Use. U.S. Food and Drug Administration 2020.
8. Ptasinska A, Whalley C, Bosworth A, Poxon C, Bryer C, Machin N, Grippon S, Wise EL, Armson B, Howson ELA and others. Diagnostic accuracy of Loop mediated isothermal amplification coupled to Nanopore sequencing (LamPORE) for the detection of SARS-CoV-2 infection at scale in symptomatic and asymptomatic populations. medRxiv 2020.
9. Wu Q, Suo C, Brown T, Wang T, Teichmann SA, Bassett AR. INSIGHT: A population-scale COVID-19 testing strategy combining point-of-care diagnosis with centralized high-throughput sequencing. Science Advances 2021;7(7):eabe5054.
10. Yelagandula R, Bykov A, Vogt A, Heinen R, Özkan E, Strobl MM, Baar JC, Uzunova K, Hajdusits B, Kordic D and others. SARSeq, a robust and highly multiplexed NGS assay for parallel detection of SARS-CoV2 and other respiratory infections. medRxiv 2020.
11. Hossain A, Reis AC, Rahman S, Salis HM. A Massively Parallel COVID-19 Diagnostic Assay for Simultaneous Testing of 19200 Patient Samples. Google Docs 2020.
12. Bloom JS, Jones EM, Gasperini M, Lubock NB, Sathe L, Munugala C, Booeshaghi AS, Brandenberg OF, Guo L, Boocock J and others. Swab-Seq: A high-throughput platform for massively scaled up SARS-CoV-2 testing. medRxiv : the preprint server for health sciences 2020.
13. Bruce EA, Huang M-L, Perchetti GA, Tighe S, Laaguiby P, Hoffman JJ, Gerrard DL, Nalla AK, Wei Y, Greninger AL and others. Direct RT-qPCR detection of SARS-CoV-2 RNA from patient nasopharyngeal swabs without an RNA extraction step. PLOS Biology 2020;18(10):e3000896.
14. Smyrlaki I, Ekman M, Lentini A, Sousa NRd, Papanicolaou N, Vondracek M, Aarum J, Safari H, Muradrasoli S, Rothfuchs AG and others. Massive and rapid COVID-19 testing is feasible by extraction-free SARS-CoV-2 RT-PCR. Nature Communications 2020;11(1):4812.
15. MacKay MJ, Hooker AC, Afshinnekoo E, Salit M, Kelly J, Feldstein JV, Haft N, Schenkel D, Nambi S, Cai Y and others. The COVID-19 XPRIZE and the need for scalable, fast, and widespread testing. Nature Biotechnology 2020;38(9):1021-1024.
16. Esbin MN, Whitney ON, Chong S, Maurer A, Darzacq X, Tjian R. Overcoming the bottleneck to widespread testing: A rapid review of nucleic acid testing approaches for COVID-19 detection. RNA (New York, N.Y.) 2020:rna.076232.120.
17. Arnaout R, Lee RA, Lee GR, Callahan C, Yen CF, Smith KP, Arora R, Kirby JE. SARS-CoV2 Testing: The Limit of Detection Matters. bioRxiv 2020:2020.06.02.131144.
18. SARS-CoV-2 Reference Panel Comparative Data. U.S. Food and Drug Administration 2020.

19. Real-Time RT-PCR Panel for Detection, 2019-Novel Coronavirus - Instructions for Use. Center for Disease Control and Prevention 2020.
20. Bar-On YM, Flamholz A, Phillips R, Milo R. SARS-CoV-2 (COVID-19) by the numbers. eLife 2020;9:e57309.
21. Bar-On YM, Flamholz A, Phillips R, Milo R. SARS-CoV-2 (COVID-19) by the numbers. Elife 2020;9.
22. Arnaout R, Lee RA, Lee GR, Callahan C, Yen CF, Smith KP, Arora R, Kirby JE. SARS-CoV2 Testing: The Limit of Detection Matter. bioRxiv 2020.
23. Zhang DY, Winfree E. Control of DNA strand displacement kinetics using toehold exchange. Journal of the American Chemical Society 2009;131(47):17303-14.
24. PerkinElmer Inc. New Coronavirus Nucleic Acid Detection Kit Instructions for Use. U.S. Food and Drug Administration 2020.
25. PerkinElmer Inc. PerkinElmer New Coronavirus Nucleic Acid Detection Kit Instructions for Use. U.S. Food and Drug Administration 2020.
26. Hologic. Panther Fusion SARS-CoV-2 Assay Instructions for Use. U.S. Food and Drug Administration 2020(AW-21159-001 Rev. 002).
27. Roche Molecular Systems Inc. cobas SARS-CoV-2 Instructions for Use (Doc Rev. 5.0). U.S. Food and Drug Administration 2020.
28. Ludwig KU, Schmithausen RM, Li D, Jacobs ML, Hollstein R, Blumenstock K, Liebing J, Słabicki M, Ben-Shmuel A, Israeli O and others. LAMP-Seq enables sensitive, multiplexed COVID-19 diagnostics using molecular barcoding. Nat Biotechnol 2021;39(12):1556-1562.
29. Broad Institute. COVID-19 Diagnostic Processing Dashboard. https://covid19-testing.broadinstitute.org/ 2021.
30. Bull RA, Adikari TN, Ferguson JM, Hammond JM, Stevanovski I, Beukers AG, Naing Z, Yeang M, Verich A, Gamaarachchi H and others. Analytical validity of nanopore sequencing for rapid SARS-CoV-2 genome analysis. Nat Commun 2020;11(1):6272.

Acknowledgements

We thank our collaborators at the Springer and Sabeti labs for sharing clinical specimens and RT-qPCR data, in particular Sarah Boswell, Jason Qian, Zhixiang Lu, Cameron Myhrvold, Jon Aristi Sanz for their help. We thank Michael Springer, David Walt, Sri Kosuri, Rebecca Ward, Ying Lu, Igor Kozlov, Thomas Albert, Peng Yin, Feng Xuan, Jenny Tam, Gabriel Filsinger, Dmitry Ter-Ovanesyan for helpful discussions. We thank Samamtha Keough, Derek Barton, Sibylle Kelleher, Robert Gage from the Department of Systems Biology, and Robert Steen, Ashley Ciulla, Justin Curran from the Biopolymers Facility at Harvard Medical School, for their earnest help, especially during the COVID lockdown period.

Funding: We thank the Department of Systems Biology at Harvard Medical School for financial support for this research.

Author contributions: M.D., G.M.C. and M.W.K. conceived of the research. M.D. designed and performed the experiments. W.M., H.K. and M.S. helped with development of one-pot RT reaction; M.D., G.M.C. and M.W.K. wrote the manuscript, all authors approved the manuscript.

Competing interests: M.D., G.M.C. and M.W.K. have filed a patent application based on this research.

Data and materials availability: Raw qPCR and sequencing data and analysis are available upon request from corresponding authors.

Supplementary Materials

Supplementary Information is provided as a separate PDF file, with the following contents:

Figs. S1 to S9

Tables S1, S3 to S9

Table S2 is provided as a separate Excel file.